IOP PUBLISHING PHYSIOLOGICAL MEASUREMENT

Physiol. Meas. **31** (2010) S183–S198 doi:10.1088/0967-3334/31/10/S03

Insulating electrodes: a review on biopotential front ends for dielectric skin–electrode interfaces

Enrique Spinelli and Marcelo Haberman

LEICI—Departamento de Electrotecnia, Universidad Nacional de La Plata and Consejo de Investigaciones Científicas y Técnicas (CONICET), CC 91 (1900) La Plata, Argentina

E-mail: spinelli@ing.unlp.edu.ar

Received 21 November 2009, accepted for publication 18 March 2010
Published 10 September 2010
Online at stacks.iop.org/PM/31/S183

Abstract

Insulating electrodes, also known as capacitive electrodes, allow acquiring biopotentials without galvanic contact with the body. They operate with displacement currents instead of real charge currents, and the electrolytic electrode–skin interface is replaced by a dielectric film. The use of insulating electrodes is not the end of electrode interface problems but the beginning of new ones: coupling capacitances are of the order of pF calling for ultra-high input impedance amplifiers and careful biasing, guarding and shielding techniques. In this work, the general requirements of front ends for capacitive electrodes are presented and the different contributions to the overall noise are discussed and estimated. This analysis yields that noise bounds depend on features of the available devices as current and voltage noise, but the final noise level also depends on parasitic capacitances, requiring a careful shield and printed circuit design. When the dielectric layer is placed on the skin, the present-day amplifiers allow achieving noise levels similar to those provided by wet electrodes. Furthermore, capacitive electrode technology allows acquiring high quality ECG signals through thin clothes. A prototype front end for capacitive electrodes was built and tested. ECG signals were acquired with these electrodes in direct contact with the skin and also through cotton clothes 350 μm thick. They were compared with simultaneously acquired signals by means of wet electrodes and no significant differences were observed between both output signals.

Keywords: insulating electrodes, active electrodes, non-contact measurements

(Some figures in this article are in colour only in the electronic version)

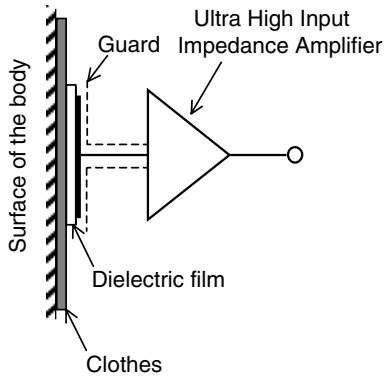

Figure 1. General structure of a capacitive coupled electrode. Biopotentials are picked up through a dielectric electrode/skin interface.

1. Introduction

Biopotentials are one of the most important tools in medical diagnosis. They are simple to acquire, they do not demand high cost equipment and there is a lot of accumulated medical experience in the interpretation of these signals. In the early years of this technique, needle electrodes or skin abrasion was often required to obtain high quality records. The continuous advances of the amplifier technology allow acquiring better and better quality signals reducing invasivity, thus increasing patient comfort. This means improving human quality of life: perhaps the main objective of the technology.

The most commonly used method to pick up biopotentials is by means of 'wet' electrodes. This approach involves metal electrodes and an electrolyte which could be a liquid, a paste or more presently a gel. These electrodes work as transducers, transforming the ionic currents inside the body into electronic currents feasible to be processed by electronic devices. This process occurs in the electrode–skin interface, which can be split into two interfaces: electrode/electrolyte and electrolyte/skin. The former does not significantly contribute to the overall signal noise, which is imposed by the electrolyte/skin interface (Huigen *et al* 2002, Fernandez and Pallas-Areny 2000). This noise exceeds that expected by the real part of the electrode–skin impedance, thus showing its electrochemistry origin (Huigen *et al* 2002). Also, dc offset voltages up to hundreds of millivolts appear in the metal/electrolyte interface, jeopardizing the amplifier input range and imposing design restrictions (Spinelli *et al* 2003).

Nowadays, current disposable pre-gelled electrodes let us obtain high resolution biopotential records by using surface electrodes and without skin abrasion. However, this technique relies on an electrolyte gel, which could produce irritation and damage on the skin of neonates (Kato *et al* 2006) and degrades signal quality when used for long-term monitoring (Matthews *et al* 2007). Also, the electrolyte hinders the use of high density surface electrode arrays, because it produces short-circuits between electrodes. Capacitive electrodes solve these problems (Clippingdale *et al* 1994, Oehler *et al* 2008b, Harland *et al* 2005) because no electrolyte is used instead of a dielectric film (figure 1). They are easy to install, appropriate for long-term monitoring and intrinsically safe, because no real charge transfer occurs between the body and the acquisition system.

Capacitive electrode technology permits us to pick up biopotentials through clothing, leading to very wearable biomedical devices (Matthews *et al* 2005, Matthews *et al* 2007, Yu *et al* 2009). It also provides a way to health monitoring in domestic environments, by installing

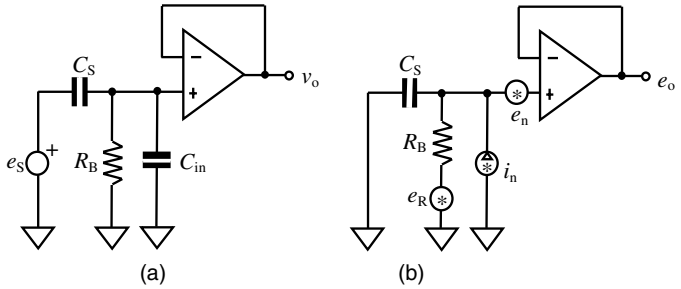

Figure 2. (a) Simplified scheme of the front-end circuit and (b) including the main noise sources.

capacitive electrodes in chairs (Lim *et al* 2006), beds (Lim *et al* 2007) and even in toilet seats (Baek *et al* 2008).

The idea of insulating electrodes is old but current. In the 1960s, Richardson (1967) managed to acquire surface biopotential by using insulating electrodes built with a very thin aluminum oxide coating as dielectric film. These electrodes, placed on the skin, provided very high coupling capacitances (several nF), thus relaxing the amplifier's requirements and admitting the implementation of this technique with available devices at that time. The current amplifiers allow relaxing coupling requirements, providing high quality records under worse conditions, as those found by acquiring biopotentials through clothing, hair or through thick dielectric layers (Prance *et al* 2000, Harland *et al* 2000, Matthews *et al* 2007).

When biopotentials are picked up through clothes, coupling capacitances are of a few pF (Ueno *et al* 2007, Lim *et al* 2006, Kim *et al* 2005) increasing up to hundreds of pF when the insulation film is directly placed over the skin. In order to ensure a low frequency response and to avoid signal attenuation, such capacitances call for ultra-high input impedance amplifiers (in the order of TΩ). Also, when using insulating electrodes, a path for the amplifier's bias current must be provided because it cannot flow through the patient, as is the case when wet electrodes are used.

The design of low noise amplifiers for insulating electrodes, fulfilling biomedical standards regarding frequency and transient response, is a fascinating challenge. It consists in achieving low noise levels in front of source impedances of a few pF, preserving input impedances of TΩ while providing paths for the amplifier's bias currents. Different approaches to deal with these issues will be analyzed herein.

2. Front ends for insulating electrodes

A front end for insulating electrodes basically consists of an ac coupled voltage follower as shown in the simplified scheme of figure 2(a). The main issue is to deal with very small source capacitances C_S, because they require ultra-high input impedances. Also, a path for the amplifier's bias current must be provided, thus forcing inclusion of a grounded resistor R_B as is indicated in figure 2(a). Moreover, high value resistors R_B present high thermal noise, which will not be effectively short-circuited through C_S as happens in standard applications.

The input impedance, formed by R_B and the input capacitance C_{in} (figure 2), must be much larger than the source impedance imposed by C_S, in order to avoid signal attenuation and mainly to achieve a gain independent of the coupling capacitance C_S. Because of the capacitive voltage divider formed by C_S and C_{in}, a very low input capacitance C_{in} is required. Otherwise, due to the potential divider effect (Metting Van Rijn *et al* 1990), a poor rejection to interference and motion artifacts results.

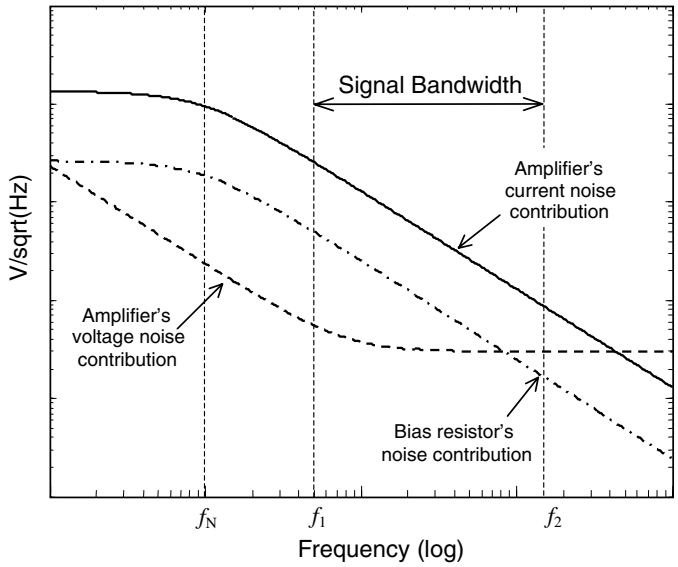

Figure 3. Different noise contributions to the overall noise power spectral density: amplifier current noise (solid line), amplifier voltage noise (dashed line) and bias resistor noise (dashed/dot line).

Regarding C_S values of a few pF (10 pF implies an impedance around 1 GΩ at 10 Hz), input capacitances C_{in} of fF and R_B of TΩ are required to avoid signal attenuation and to achieve time constants of seconds, which are required, for example to acquire ECG signals (AAMI 1999). The ultra-high R_B values demand special bias circuits, whereas the low C_{in} values required call for careful input capacitance reduction techniques.

In summary, the key issues are ultra-high impedance bias circuits, input capacitance reduction and achievement of low noise levels dealing with high value R_B and small coupling capacitances C_S.

2.1. Noise analysis

A simplified scheme of a front end for capacitive electrodes, including the main noise sources, is shown in figure 2(b). The resistor noise is denoted as e_R whereas e_n and i_n represent, respectively, the voltage and the current noise of the amplifier. Solving this circuit, the output noise e_o results in

$$e_o^2 = e_R^2 \frac{1}{1 + (2\pi R_B C_S f)^2} + i_n^2 \frac{R_B^2}{1 + (2\pi R_B C_S f)^2} + e_n^2 \tag{1}$$

Denoting the −3 db noise cut-off frequency as f_N:

$$f_N = \frac{1}{2\pi R_B C_S}, \tag{2}$$

equation (1) reduces to

$$e_o^2 = e_R^2 \frac{1}{1 + (f/f_N)^2} + i_n^2 \frac{R_B^2}{1 + (f/f_N)^2} + e_n^2. \tag{3}$$

A typical curve of the overall output noise and the contributions of each term in (3) is shown in figure 3. The low frequency noise values e_R and $i_n R_B$ are very large, around 100 μV Hz$^{-1/2}$

for $R = 1$ TΩ and i_n as low as 0.1 fA Hz$^{-1/2}$. In order to reduce these noise contributions to acceptable values, the noise cut-off frequency f_N must be considerably below the signal bandwidth and, in this frequency range, (3) can be approximated by

$$e_o^2 \approx e_R^2 (f_N/f)^2 + i_n^2 R_B^2 (f_N/f)^2 + e_n^2. \tag{4}$$

Replacing e_R by the Nyquist expression $\left(e_R^2 = 4kTR_B\right)$ and f_N by (2) results in

$$e_o^2 \approx \frac{kT}{(\pi C_S f)^2}\frac{1}{R_B} + \frac{i_n^2}{(2\pi C_S f)^2} + e_n^2 \tag{5}$$

$$e_o^2 \approx \frac{1}{(\pi C_S f)^2}\left(\frac{kT}{R_B} + \frac{i_n^2}{4}\right) + e_n^2. \tag{6}$$

The last term, due to operational amplifier (OA) voltage noise, as well as eventual spontaneous EMG potential under the electrode area, will also be present in wet electrodes measurements (Huigen *et al* 2002, Matthews *et al* 2005). The analysis that follows focuses on the first two terms. They decrease with frequency and could be regarded as an 'excess noise' against the use of wet electrodes. The resistor noise equals the amplifier current noise contributions for $R_B = R_{B,C}$ given by

$$R_{B,C} = 4kT/i_n^2. \tag{7}$$

Considering $i_n = 1$ fA Hz$^{-1/2}$ and $T = 310$ K, $R_{B,C} = 17$ GΩ results. In general, for R_B values lower than tens of GΩ, the resistor noise is the main contribution and, according to (6), the output noise decreases with R_B as was reported in Prance *et al* (2000). On the other hand, for the R_B values of a few TΩ or more, the resistor noise is negligible with respect to the amplifier current noise contribution, even with i_n as low as 0.1 fA Hz$^{-1/2}$, as was stated by Sullivan *et al* (2007) and Matthews *et al* (2005).

The present available devices have bias current below 1 pA and, more important, very low current noise, for instance 0.1 fA Hz$^{-1/2}$ for the OPA129 and 0.22 fA Hz$^{-1/2}$ for the AD549. Figure 4 shows the noise bound according to (6) for the OPA129 with $R_B = 10$ TΩ and $C_S = 10$ pF. In this case, even with this low coupling capacitance, the expected noise power spectral density (PDS) is really low: around 200 nV Hz$^{-1/2}$ at 10 Hz, which is slightly larger than the OA voltage noise and comparable to low noise wet electrode features (Harland *et al* 2003).

As can be observed in (6), noise reduces with C_S; this is with the electrode area. Therefore, for a given OA, noise can be reduced by increasing electrode size, as happens when wet electrodes are used (Huigen *et al* 2002).

Expression (6) corresponds to the output noise PDS. The root mean square (RMS) noise of the front end can be obtained by integrating (6) over a given bandwidth $BW = f_1 - f_2$ as

$$E_o^2 = \int_{f_1}^{f_2}\left(\frac{kT}{(\pi C_S f)^2}\frac{1}{R_B} + \frac{i_n^2}{(2\pi C_S f)^2} + e_n^2\right) \mathrm{d}f. \tag{8}$$

Considering that BW usually covers few decades, (8) results in

$$E_o^2 \approx \frac{kT}{(\pi C_S)^2}\frac{1}{R_B f_1} + \frac{i_n^2}{(2\pi C_S)^2}\frac{1}{f_1} + E_n^2, \tag{9}$$

where f_1 is the signal lower cut-off frequency. It is important to note that the output noise E_o does not depend on the signal bandwidth but on f_1, which clearly shows that noise can be reduced by increasing the cut-off frequency f_1: a usual practice in capacitive electrodes (Lim *et al* 2006, Baek *et al* 2008). Cut-off frequencies of up to 8 Hz have been used for heart rate detectors (Wu and Zhang 2008), but f_1 must be of tenths of hertz in order to fulfill medical standards, thus keeping the same diagnostic capacity of wet electrodes (AAMI 1999).

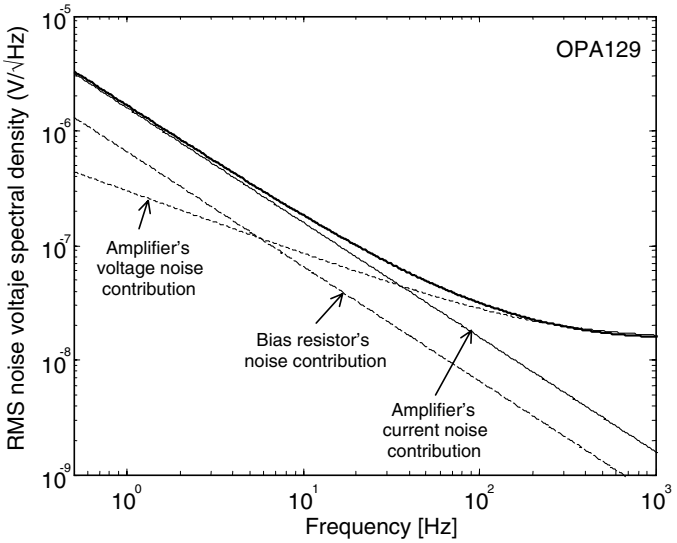

Figure 4. Overall estimated noise (bold solid line) for an operational amplifier OPA129 with $R_B = 10$ TΩ and $C_S = 10$ pF. The different noise components are also indicated: amplifier current noise (solid fine line), bias resistor noise (dashed line) and amplifier voltage noise (dotted line).

2.2. Bias circuits

The currently available devices present bias currents as low as tens of fA. However, a path to ground for this current must be provided because, left unattended, it integrates with the capacitance C_S leading the OA outside its range of operation.

There are many ways to provide bias paths, but all of them work like a grounded high value resistor R_B (almost inside the signal bandwidth). The bias resistor R_B should be as high as possible in order to avoid degrading the input impedance and also, as is described above, to reduce output noise. The maximum admissible value $R_{B,MAX}$ is limited by the amplifier bias current and power supply voltages. Considering a rail-to-rail OA, it is given by

$$R_{B,MAX} < \frac{V_{CC}}{i_{BIAS}}. \tag{10}$$

For example, an OA with $i_{BIAS} = 1$ pA, powered by a ±5 V voltage supply, admits R_B values up to 5 TΩ. This resistor is not required to be very precise, but it must be lower than $R_{B,MAX}$ in order to ensure a proper dc operation voltage and high enough to ensure a given low cut-off frequency. The offset voltage due to i_{BIAS} flowing on R_B may be of a few volts, but it can be removed when the signal bandwidth is limited between f_1 and f_2 or by a negative feedback of the low frequency components (Clippingdale *et al* 1994, Clark *et al* 2003).

In some applications, like heart rate detectors, low R_B values (of a few GΩ) are usually used. In this case the signal low cut-off frequency f_1 is found to be of several hertz and the amplifier gain becomes strongly dependent on the coupling capacitance, because the input impedance is not high enough (Lim *et al* 2006, Wu and Zhang 2008, Ueno *et al* 2007). These capacitive electrodes are robust and they recover quickly from artifacts, but introduce low frequency distortion on the ECG signals, thus limiting its diagnostic capability.

High value resistors can be 'simulated' by positive feedback (bootstrapping), but their noise is greater than that of a real resistor of the same value (Lanyi 2001). Nowadays, surface mount resistors up to 1 TΩ are commercially available (IMS 2009) and 'real' resistors can be

used. However, there are some other approaches to achieve the R_B values of the order of TΩ. Richardson and Lopez (1970) and Yu *et al* (2009) used the reverse current of signal diodes to provide the bias current, Sullivan *et al* (2007) omitted the resistor R_B but provided a 'reset' feature to recover the OA when i_{BIAS} led it to saturation and Prance *et al* (2000) proposed a carefully designed and built a printed circuit board (PCB) that allows us to keep the amplifier in operation for hours without a lumped resistor R_B: the PCB insulation leakage is enough to provide a path for the extremely low bias current of the used amplifier ($i_{BIAS} = 100$ fA for the INA116).

In this paper, a similar approach to that in Prance *et al* (2000) was used to obtain the experimental data of the last section; given that insulation resistances are of the order of TΩ, the insulation resistance itself was used as R_B. Two techniques were tested to implement R_B: (1) by placing few turns of insulated wire rolled-up on the non-inverter pin of the amplifier (this pin was not soldered to the board) and (2) with a grounded PCB line close to other trace connected at the mentioned pin. The first alternative gives the best results, it allows easily adjusting R_B by adding additional turns and it results in lower capacitances to ground, but it is more 'homemade' than the PCB approach. On the other hand, the second option requires some trial-and-error steps to achieve a required PCB insulation leakage resistor for a given PCB material and R_B also depends on PCB conditions as clearness and dryness.

2.3. Reduction of input capacitance effects

Operational amplifiers (OAs) with input capacitances of a few pF are available, but these C_{in} values are too high to acquire biopotentials through a T-shirt (C_S of a few tens of pF). Moreover, low voltage noise CMOS OAs present large input capacitances (up to tens of pF), because they are built with large area transistors (National Instrument 2008).

The capacitance C_{in}, which comprises OA common mode input capacitance and also stray PCB capacitances to ground, is difficult to reduce but its effects can be avoided by guarding, neutralization and bootstrapping techniques.

2.3.1. Guarding. By guarding, the effects of stray capacitances between the amplifier input and the remaining circuit can be avoided. It consists in surrounding this node by a guard which is driven to the same node potential by a low output impedance circuit. In this way, no potential difference appears on the mentioned capacitances (indicated as C_{SH} in figure 5(a)) and no current flows through them. In this same way, guarding avoids spurious resistive paths, thus preserving R_B. The mentioned C_{SH} capacitance also comprises the differential mode input capacitance of the OA.

The active guarding scheme involves a positive feedback through C_{SH}. In general, the capacitance between guard and ground is small; it does not impose a significant load to the OA and no stability problems arise when a properly compensated OA is used (Spinelli and Reverter 2010). However, the OA voltage noise e_n is amplified at the output as

$$e_o = e_n C_{SH}/C_S. \tag{11}$$

To implement the guarding scheme, a unity gain front end is required. It does not impose a serious limitation, because no gain is needed at this stage: the front-end function is to transform ultra-high input impedance to low output impedance. Gain can be achieved by a subsequent bipolar technology amplifier whose voltage noise can be made negligible compared to the front-end noise. This later must be CMOS in order to achieve low current noise levels.

2.3.2. Neutralization. Guarding compensates for the effects of many parasitic capacitances and resistive losses at the amplifier input, but the amplifier input capacitance, as well the

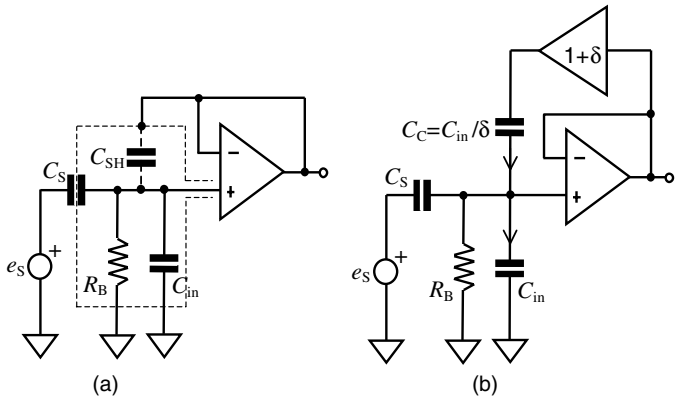

Figure 5. Simplified circuits of input capacitance reduction techniques. (a) Equivalent circuit of active guarding. (b) Neutralization of C_{in} by using a positive feedback.

capacitance associated with R_B, remains unchanged. These grounded capacitances can be compensated for by 'neutralization'. This old technique, historically and extensively used for micropipette electrodes (Amatniek 1958), can be applied to solve present biomedical problems. It consists in providing, by a positive feedback, a current that equals the current flowing on C_{in}. The scheme, shown in figure 5(b), involves an amplifier with a gain $(1 + \delta)$ and a feedback capacitance C_C that verifies

$$C_C = C_{in}/\delta. \tag{12}$$

In this way, by adjusting C_C or δ, the current on C_C may exactly compensate for the current on C_{in}, thus neutralizing the effect of this capacitance. This technique solves the C_{in} problem, but as the 'difficulty-conservation principle' predicts, another problem arises: the neutralization circuit amplifies the voltage noise of the OA (Amatniek 1958). Solving the circuit regarding the noise of the voltage follower and the voltage noise of the feedback OA (e_{1n}, e_{2n}, respectively) results in

$$e_o = \sqrt{e_{1n}^2(1 + (1 + 1/\delta)C_{in}/C_S)^2 + e_{2n}^2((1 + 1/\delta)C_{in}/C_S)^2}. \tag{13}$$

Noise reduces as δ increases, but in general δ values around the unity are adopted to avoid very small C_C values. Under this condition, and assuming the same noise voltage e_n for both OAs, (13) becomes

$$e_o = e_n\sqrt{1 + 4C_{in}/C_S + 8(C_{in}C_S)^2}, \tag{14}$$

which clearly shows that the ratio C_{in}/C_S amplifies the OA noise e_n.

2.3.3. Power supply bootstrapping. The amplifier input capacitance is not really grounded. It is referred to the power supply rails (OAs do not have a 'ground' pin). So, if power supplies follow the follower's input, no current flows through these capacitances and its effects are avoided. This technique, known as 'power supply bootstrapping' (Lanyi and Pisani 2002, Prance *et al* 2000), allows compensation for the input capacitance without adjustment (Kootsey and Johnson 1973). However, it demands several components and is not well suited for capacitive electrodes, where compact implementation is desired. Moreover, this technique compensates for the OA input capacitance, but is not able to compensate for the grounded capacitance associated with R_B.

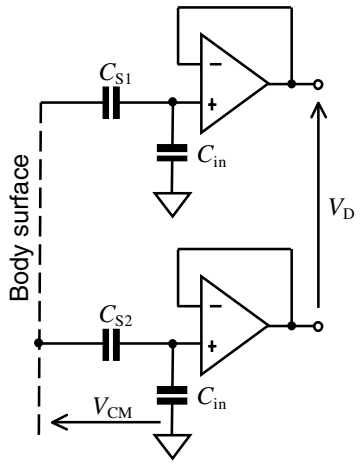

Figure 6. Scheme of capacitive electrodes in differential configuration. The common mode voltage V_{CM} is transformed to differential mode signal V_D due to unbalances between the coupling capacitances C_{S1} and C_{S2}.

3. Power line interference rejection

Capacitive electrodes are very susceptible to power line interference due to the ultra-high impedances involved (Kim and Park 2008). In order to reduce interference to acceptable levels, the front-end circuit must be placed in the electrode itself. This technique, known as 'active electrodes', sometimes used to improve interference rejection in wet electrodes, is mandatory for capacitive electrodes.

Once the electrode containing the front end is properly shielded, the main interference contribution that remains is due to the common mode voltage V_{CM} imposed by the power line. This common mode potential produces a differential mode voltage V_D as a result of unbalanced coupling capacitances of different channels (figure 6). This differential voltage that will not be rejected by a subsequent differential amplifier is given approximately by (Metting Van Rijn *et al* 1990)

$$V_D = V_{CM} \frac{\Delta Z_E}{Z_C}, \tag{15}$$

ΔZ_E being the electrode impedance unbalance and Z_C the amplifier common mode input impedance. In the capacitive electrodes case, (15) results in

$$V_D = V_{CM} 2 \frac{C_{in}}{C_S} \frac{\Delta C_S}{C_S}, \tag{16}$$

where $\Delta C_S = C_{S1} - C_{S2}$ denotes the unbalance between the coupling capacitances of each channel. Then, to reduce this interference, the common mode voltage V_{CM} and the input capacitance C_{in} should be made as low as possible. The coupling capacitance C_S imposes the measurement conditions and cannot be managed by design.

As was previously described, the effective input capacitance C_{in} can be reduced by using active techniques. The common mode voltage V_{CM} can be reduced, connecting the patient to the amplifier ground by means of a low impedance path. It can be implemented by a large area plate capacitor (Lim *et al* 2007) or by a wet electrode (Oehler *et al* 2008a). The last option also prevents the accumulation of electrostatic charges (Casas and Pallas-Areny 2007)

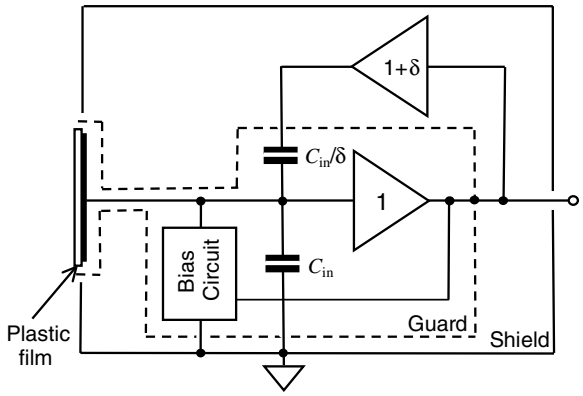

Figure 7. Block diagram of the front end used to obtain the experimental data.

whereas the placement of just one wet electrode does not impose a serious inconvenience for a multi-channel system with a large number of capacitive electrodes (Oehler *et al* 2008a). Another effective way to reduce V_{CM} is by means of a common mode negative feedback. This strategy, known as driven right leg circuit (DRL), extensively used for wet electrodes, has been successfully tested for fully capacitive coupled systems (Kim *et al* 2005, Steffen *et al* 2007).

4. Experimental results

A capacitive electrode for ECG measurements was built and tested. It was implemented by using a general-purpose quad CMOS opamp (TLC2274 of Texas Instruments) in order to achieve low-cost implementation with a reduced number of parts. It presents a voltage noise of 50 nV $Hz^{-1/2}$ at 10 Hz, a current noise of 0.6 fA $Hz^{-1/2}$ and a bias current of 1 pA; these features are not as good as those of OPA129 or AD549 but they are good enough to acquire ECG signals.

The bias resistor, implemented by insulation leakage, was of around 3 TΩ. A low frequency negative feedback was included in order to stabilize dc operation point (Clippingdale *et al* 1994, Clark *et al* 2003) and also guarding and neutralization circuits were used to keep low C_{in} values. The general scheme of the built capacitive electrode is shown in figure 7.

The electrode, shown in figure 8(a), has a diameter of 30 mm and was made of a standard dual layer printed circuit board. One layer is in contact with the dielectric film and the other supports components whereas the remaining cooper area implements the guard.

The electrode was insulated by a plastic auto-adhesive film. Coupling capacitances were measured using a potential-divider-based method (Prance *et al* 2000) with 1 kHz square wave resulting $C_S = 240$ pF when the electrode is placed on the skin and $C_S = 20$ pF when it was applied through a 350 μm thick cotton T-shirt. By the same method, using a capacitor $C_S = 10$ pF, the neutralization of each electrode was individually adjusted to achieve unity gain.

The power spectral density noise of the front end, experimentally obtained for $C_S = 10$ pF and $C_S = 100$ pF, is shown in figure 9. This figure also includes (in dashed lines) the theoretical PSD predicted by (6) for the TLC2274 parameters. It can be

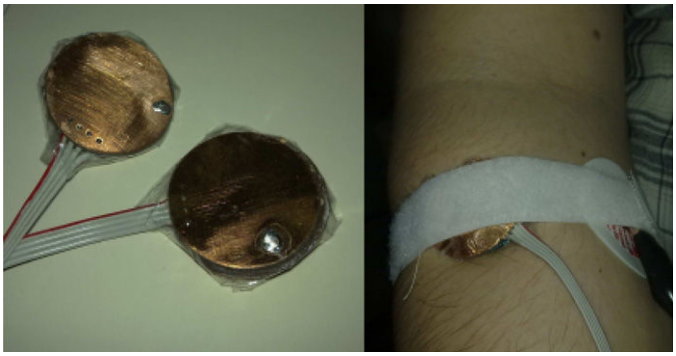

Figure 8. (a) 'Handmade' capacitive electrodes used in the test. (b) Experimental setup for the first subject, where capacitive electrodes were placed in each arm directly over the skin.

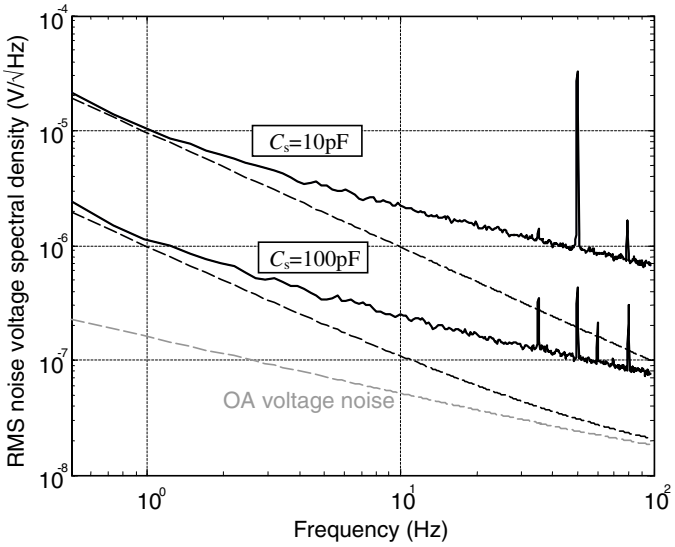

Figure 9. Power spectral density (PSD) noise of the front end for two coupling capacitances: $C_S = 10$ pF and $C_S = 100$ pF. Solid lines correspond to experimental PSD data and dashed lines in black to theoretical PSD according to (6) for the TLC2274 operational amplifier. The gray dashed line indicates OA voltage noise.

observed that, for low frequencies, the noise matches to that foreseen by (6), whereas for high frequencies, it looks like an amplified version of the OA voltage noise e_n. It can also be observed that this noise increases as C_S reduces, which agrees with the noise behavior of the neutralization and guarding circuit described by (11) and (13). It is worth noting that the measured noise significantly exceeds the values predicted by these equations. Another hidden noise source with similar behavior may be responsible for this difference.

The frequency responses of the electrodes for $C_S = 10$ pF and $C_S = 100$ pF were experimentally measured by a frequency sweep resulting in the data shown in figure 10(a).

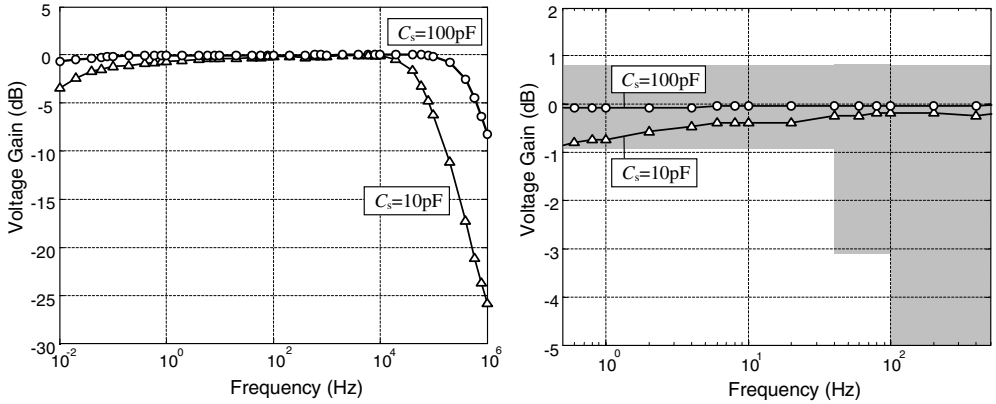

Figure 10. Frequency response of the built amplifier for two coupling capacitances: $C_S = 10$ pF (triangles connected by lines) and $C_S = 100$ pF (circles connected by lines). Detail is also presented including (in gray) the limits imposed by the AAMI ECG standard. This requirement are fulfilled for $C_S = 100$ pF and also for $C_S = 10$ pF.

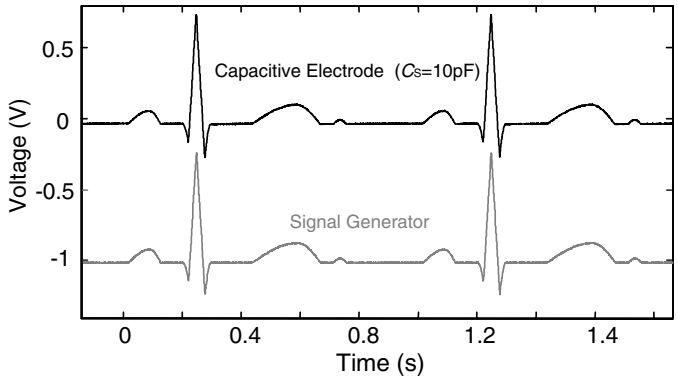

Figure 11. Response of the capacitive electrodes (in black) to a simulated ECG input signal (in gray). A coupling capacitance $C_S = 10$ pF was used for this test.

Detail is presented in figure 10(b), which allows observing that requirements of the AAMI ECG standard (AAMI 1999) are fulfilled, even with a coupling capacitance of 10 pF (a condition representative of acquiring ECG through a T-shirt). In order to complete the electrode's test under well-known conditions, a simulated 1 Hz ECG signal (HP 33120A) with a coupling capacitance of 10 pF was used as input, resulting in the records shown in figure 11. No difference can be observed between the input signal and the capacitive electrode's output.

Finally, to test the electrodes under real conditions, ECG signals were acquired over two subjects with capacitive electrodes and simultaneously by wet electrodes (disposable 3M 2223) using an ECG acquisition system that fulfill the AAMI standard (Spinelli *et al* 2003).

In the first test, both electrodes (capacitive and wet) were placed on the inner arm over the skin (figure 8(b)), resulting in the signals shown in figure 12. No significant differences can be observed between the ECG provided by capacitive electrodes (in black) and that picked up

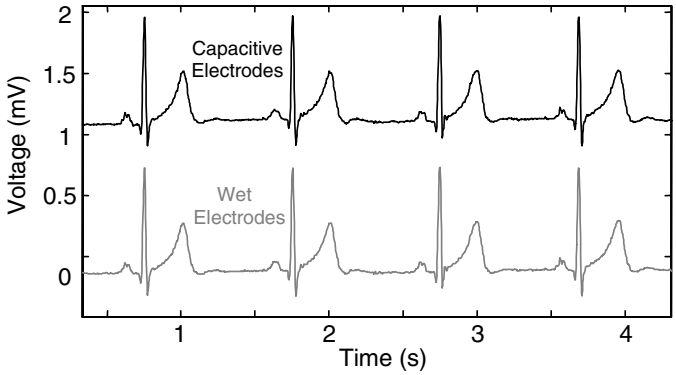

Figure 12. Waveforms of signals obtained on the first subject. Two differential channels were taken at the same time in the same location: one using capacitive electrodes (upper signal) and other by wet electrodes (lower signal). No significant differences are seen.

Figure 13. Experimental setup on the second subject's chest. Capacitive electrodes were placed over a 350 μm thick cotton T-shirt. Disposable pre-gelled electrodes were placed near these locations under the T-shirt.

by standard wet electrodes (in gray). Tapping on the capacitive electrodes, a good rejection to motion artifacts was observed, similar to that of wet electrodes as described in Searle and Kirkup (2000).

The second test consisted of placing the capacitive electrodes over a T-shirt (figure 13). The ECG signals obtained in this case are shown in figure 14. The signal quality provided by the insulating electrodes is comparable to that achieved by wet electrodes, but the breathing artifacts of capacitive electrodes are quite high (around 2 mV). This is common when biopotentials are acquired through small capacitances C_S such as through clothing or thick dielectric layers (Clippingdale *et al* 1994). The record in figure 15, obtained when the subject avoided breathing (apnea), shows that the signal quality by using capacitive electrode working through a T-shirt is practically identical to that obtained from wet electrodes.

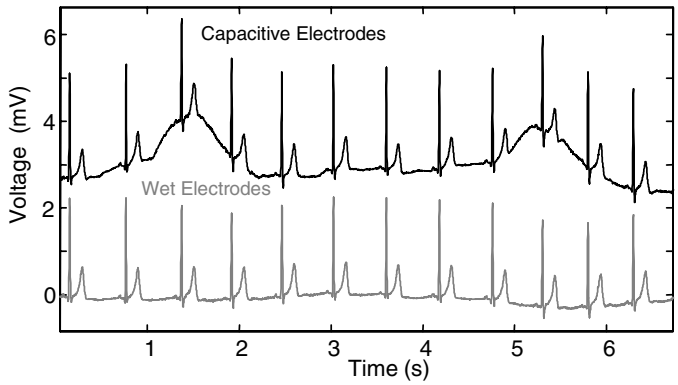

Figure 14. ECG signal acquired through a T-shirt by capacitive electrodes (upper trace) and simultaneously by wet electrodes (lower trace). Note that the breathing artifact is quite large for insulating electrodes.

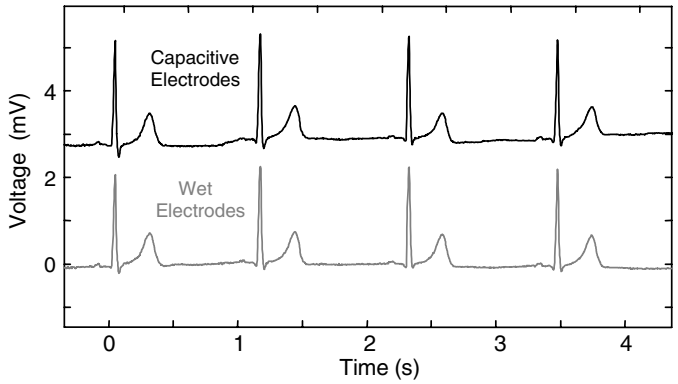

Figure 15. Waveforms of signals measured on the second subject during apnea. Two channels were taken at the same time in near locations: one using capacitive electrodes over a 350 μm thick cotton T-shirt (upper signal) and the other using wet electrodes (lower signal). No significant differences are seen.

5. Conclusion

When wet electrodes are used, the noise level depends on electrochemical processes that occur in the electrode–skin interface. On the other hand, in the case of capacitive electrodes, its noise features depend on the front-end circuit and can be improved by electronic design. In the presence of high coupling capacitances (C_S of hundreds of pF), the output noise is dominated by the voltage noise of the amplifier. If the coupling capacitance is low (few pF or less), the amplifier's current noise becomes the key parameter.

Regarding the biasing resistor R_B, its noise contribution is significant only if R_B is lower than hundreds of GΩ. In biomedical applications, time constants of several seconds are required to avoid low-frequency distortions. The resistor R_B must be of TΩ (for C_S of a few pF) and its noise contribution could be neglected. Regarding the present operational amplifiers, with noise currents as low as 0.1 fA, coupling capacitances of 100 pF are sufficient to achieve

noise levels similar to those of wet electrodes. This C_S values can be easily achieved placing a plastic dielectric layer in contact with the skin, but are difficult to achieve through clothing.

Noise bound depends on the available devices, but the final noise level also depends on parasitic capacitances, requiring a careful shield and printed circuit design. It is important to keep low input and stray capacitances, because of active capacitance reduction techniques such as guarding, bootstrapping and shielding increase noise by amplifying OA voltage noise.

A prototype amplifier was built and tested. It verified the frequency response required by the AAMI ECG standard with C_S as low as 10 pF. Also, real ECG signals were acquired by insulating electrodes in direct contact with the skin and through cotton clothes. Under both conditions, no significant differences were observed against simultaneously acquired records by wet electrodes.

Using capacitive electrodes, it is possible to acquire biopotential signals through clothing with a quality similar to that of wet electrodes. The progress made in the understanding of the technique and in the technology of the electronic devices makes it possible to think toward extending this method from research to clinical practice.

Acknowledgments

This work has been funded by the Agencia Nacional de Promoción Científica y Tecnológica (ANCyT) through Project PICT 2007-00535, Universidad Nacional de La Plata (UNLP) through Project I-127 and Consejo Nacional de Investigaciones Científicas y Técnicas (CONICET) by project PIP-112-2009-0100253. The authors also acknowledge the helpful comments of Dardo Guaraglia and the technical support of Sergio Rodriguez.

References

AAMI (Association for the Advancement of Medical Instrumentation) 1999 Ambulatory electrocardiographs *American National Standard* ANSI/AAMI EC38

Amatniek E 1958 Measurement of bioelectric potentials with microelectrodes and neutralized input capacity amplifiers *IRE Trans. Med. Electron.* **10** 3–14

Baek H, Kim J, Kim K and Park K 2008 System for unconstrained ECG measurement on a toilet seat using capacitive coupled electrodes: the efficacy and practicality *Proc. 30th Annu. Int. Conf. of the IEEE Engineering in Medicine and Biology Society* pp 2326–8

Casas O and Pallas-Areny R 2007 Electrostatic interference in contactless biopotential measurements *Proc. of the 29th Annu. Int. Conf. of the IEEE Engineering in Medicine and Biology Society* pp 2655–8

Clark T, Prance R and Harland C 2003 Electrodynamic sensors and applications *Patent Application* Publication WO 03/048789 A2

Clippingdale A, Prance R, Clark T and Watkins C 1994 Ultrahigh impedance capacitively coupled heart imaging array *Rev. Sci. Instrum.* **65** 269–70

Fernandez M and Pallas Areny R 2000 Ag–AgCl electrode noise in high-resolution ECG measurements *Biomed. Instrum. Technol.* **34** 125–30

Harland C J, Clark T D, Peters N S, Everitt M J and Stiffell P B 2005 A compact electric potential sensor array for the acquisition and reconstruction of the 7-lead electrocardiogram without electrical charge contact with the skin *Physiol. Meas.* **26** 939–50

Harland C J, Clark T D and Prance R J 2000 Electrical potential probes—new directions in the remote sensing of the human body *Meas. Sci. Technol.* **13** 163–9

Harland C J, Clark T D and Prance R J 2003 High resolution ambulatory electrocardiographic monitoring using wrist-mounted electric potential sensors *Meas. Sci. Technol.* **14** 923–8

Huigen E, Peper A and Gimbergen C A 2002 Investigation into the origin of the noise of surface electrodes *Med. Biol. Eng. Comput.* **40** 332–8

IMS (International Manufacturing Services) 2009 HCX Series Resistors available at www.ims-resistors.com

Kato T, Ueno A, Kataoka S, Hoshino H and Ishiyama Y 2006 An application of capacitive electrode for detecting electrocardiogram of neonates and infants *Proc of 28th Annu. Int. Conf. of the IEEE Engineering in Medicine and Biology Society* pp 916–9

Kim K, Lim Y and Park K 2005 Common mode noise cancellation for electrically non-contact ECG measurement system on a chair *Proc. of the 27th Annu. Int. Conf. of the IEEE Engineering in Medicine and Biology Society* pp 5881–3

Kim K and Park K 2008 Effective coupling impedance for power line interference in capacitive-coupled ECG measurement system *Proc. Int. Conf. on Technology and Applications in Biomedicine (ITAB 2008)* pp 256–8

Kootsey J and Johnson E 1973 Buffer amplifier with Femtofarad input capacity using operational amplifiers *IEEE Trans. Biomed. Eng.* **20** 389–91

Lanyi S 2001 The noise of input stages with low parasitic capacitance *Meas. Sci. Technol.* **12** 1456–64

Lanyi S and Pisani M 2002 A high input-impedance buffer *IEEE Trans. Circuits Syst.* I **49** 1209–11

Lim Y, Kim K and Park K 2006 ECG measurement on a chair without conductive contact *IEEE Trans. Biomed. Eng.* **53** 956–9

Lim Y, Kim K and Park K 2007 ECG recording on a bed during sleep without direct skin-contact *IEEE Trans. Biomed. Eng.* **54** 718–24

Matthews R, McDonald J, Fridman I, Hervieux P and Nielsen T 2005 The invisible electrode—zero prep time, ultra low capacitive sensing *Proc. of the 11th Int. Conf. on Human–Computer Interaction (HCII) (Las Vegas, NV)*

Matthews R, McDonald N J, Hervieux P, Turner P J and Steindorf M A 2007 A wearable physiological sensor suite for Unobtrusive monitoring of physiological and cognitive state *Proc. of the 29th Annu. Int. Conf. of the IEEE Engineering in Medicine and Biology Society* pp 5276–81

Metting van Rijn A, Peper A and Grimbergen C 1990 High-quality recording of bioelectric events: Part 1. Interference reduction, theory and practice *Med. Biol. Eng. Comput.* **28** 389–97

National Instruments 2008 LMP7715 datasheet available at www.national.com.

Oehler M, Neumann P, Becker M, Curio G and Schilling M 2008a Extraction of SSVEP signals of a capacitive EEG helmet for human machine interface *Proc. of the 30th Annu. Int. Conf. of the IEEE Engineering in Medicine and Biology Society* pp 4495–8

Oehler M, Schilling M, Ling V and Melhorn K A 2008b Multichannel portable ECG system with capacitive sensors *Physiol. Meas.* **29** 783–93

Prance R J, Debray A, Clark T D, Prance H, Nock M, Harland C J and Clippingdale A J 2000 An ultra-low-noise electrical-potential probe for human-boy scanning *Meas. Sci. Technol.* **11** 291–7

Richardson P C 1967 The insulated electrode: a pasteless electrocardiographic technique *Proc. Annu. Conf. on Engineering in Medicine and Biology* vol 7 pp 9–15

Richardson P C and Lopez A 1970 Electrocardiographic and bioelectric capacitive electrode *US Patent* No 3,500,823

Searle A and Kirkup L 2000 A direct comparison of wet, dry and insulation bioelectric recording electrodes *Physiol. Meas.* **21** 271–83

Spinelli E, Pallas-Areny R and Mayosky M 2003 AC-coupled front-end for biopotential measurements *IEEE Trans. Biomed. Eng.* **50** 391–5

Spinelli E and Reverter F 2010 On the stability of shield-driver circuits *IEEE Trans. Instrum. Meas.* **59** 458–62

Steffen M, Aleksandrowicz A and Leonhardt S 2007 Mobile noncontact monitoring of heart and lung activity *IEEE Trans. Biomed. Circuit Syst.* **1** 250–7

Sullivan T J, Deiss S R and Cauwenberghs G 2007 A low-noise, non-contact EEG/ECG sensor *Proc. of the IEEE Biomedical Circuits and Systems Society Conf. (BIOCAS 2007)* pp 154–7

Ueno A, Akabane Y, Kato T, Hoshino H, Kataoka S and Ishiyama Y 2007 Capacitive sensing of electrocardiographic potential through cloth from the dorsal surface of the body in a supine position: a preliminary study *IEEE Trans. Biomed. Eng.* **54** 759–66

Wu K and Zhang Y 2008 Contactless and continuous monitoring of heart electric activities through clothes on a sleeping bed *Proc. of the Int. Conf. on Technology and Applications in Biomedicine (ITAB)* pp 282–5

Yu M, Deiss S and Cauwenberghs G 2009 Non-contact low power EEG/ECG electrode for high density wearable biopotential sensor networks *Proc. 6th Int. Workshop on Wearable and Implantable Body Sensor Networks* pp 246–50